PROC. OF JSCE,
No. 211, MARCH 1973

SEISMIC DESIGN SPECTRA FOR TRENCH TYPE TUNNEL

*By Yoshinori AOKI**

1. INTRODUCTION

In a few recent years a number of subaqueous tunnels by means of the trench method have been planned and constructed in Japan. Considering the risk that subaqueous tunnels will flood in a short time even partially fractured and public traffic will suffer from serious disaster, the earthquake resistant design of tunnels is quite important. The history of the construction of subaqueous tunnels in the area where severe earthquakes occur like in Japan or in the west coast of United States of America is, however, quite new and many problems in this field are left for future research works.

Possible damage to long underground structures such as tunnels constructed by the trench method may be caused by those occasions which can be classified into following three categories; the 1st, the structure happens to be located across an active tectonic fault, then the structure may be damaged due to its activities as a result or effect of an earthquake. The 2nd, the structure is constructed in the site where some geological defects exist, then the structure may be damaged due to liquefaction of the foundation or back fill material, or due to failure of the surrounding soft soil. The 3rd, stresses induced in the structure due to dynamic deformation of the surrounding soil during an earthquake exceed the strength of structural material the structure made of.

Against the first two categories only the following countermeasure may prevent the structure from damage; that is, the tunnel route must be chosen from the result of careful geological survey so that no influential tectonic fault be across the tunnel, the tunnel route must be kept out away from the zone unstable geological configuration exist, and necessary foundation improvement work must be taken place and selected material must be used for back fill, unless otherwise the structural design in a narrow sense can not overcome the risk. Though the first and the second items are more important from the view point of the earthquake resistant of the whole facility, this paper discusses only problems in the field of the last category.

Research works concerned with the earthquake resistant design method of trench type tunnels have been done mainly from the following three aspects; the 1st is the dynamic model test. The research done by Tamura et al.[1] has made the model test practical. The 2nd is the response analysis by using an electronic computer. Researches on the development of computer programs done by Muto et al.[2], Hamada et al.[3] and Goto et al.[4] can be listed up as activities in this field. The last is the design method using design spectra. The development of a new design method[5] which the BART tunnel project was accompanied with is quite noteworthy. This design method is rather of practice, and has had a a great influence on the practical design of trench type tunnels in Japan so far. Though researches taking advantage of the earthquake swarm at Matsushiro done by Sakurai et al.[6] are not directly connected with tunnels but with underground pipelines, those are quite similar to the tunnel in some sense from the earthquake resistant design point of view and results of the researches are very suggestive.

This paper deals with a new computation method of design spectra for the earthquake-resistant design of trench type tunnels. At first the principle of the design method using spectra is recalled and its advantages and defects are discussed, then preconditions and experimental findings as the back ground of the design method are discussed. Equations to compute the spectra are led, then a tentative means to predict the bending moment at a rigid joint or the relative displacement at a flexible joint between a tunnel tube and a ventilation tower by utilizing the spectra are formulated. At last, application examples of spectra and the calculation method of problems at joints are illustrated.

* Port and Harbour Bureau, Ministry of Transport.

2. PRINCIPLE OF THE DESIGN METHOD USING SPECTRA

This design method is based on the assumptions that a light underground structure like a trench type tunnel rarely resonate with earthquakes and displacement of the structure during an earthquake is at most equal to the displacement of the surrounding ground. And a displacement transfer ratio from soil to the structure depends on the rigidities of soil and the structure. Therefore if the displacement distribution of the ground during an earthquake and the displacement transfer ratio are known, the shape of deformation of the structure during the earthquake is obtained and the earthquake resistive structure, then, can be designed.

The possibility that the design method using spectra explained hereafter results in the upper limit design, which will be discussed later, is one of the peculiarities of this design method. The distribution of the displacement of the ground during an earthquake depends upon the characteristics of the earthquake itself including surface waves, and geological and topographical configuration in the rather wide range around the point questioned. And it is quite difficult to predict an actual ground displacement distribution during an earthquake. Consequently, an upper limit design method is required in the practice.

The other advantage of this design method is that the design process is simple provided that the design spectra have been prepared in advance.

Because a single design spectrum which presumably results in the upper limit design is applied through whole part of a tunnel in its design, it is a disadvantage that some part of the tunnel may be over-designed.

Preconditions of the computation method of the design spectra are as follows;

(1) No failure of the surrounding soil or no fault activities will be considered, based on the assumption that enough attentions have already been paid when the route of the tunnel has been chosen.

(2) The spectra are computed from a strong motion accelerogram which is assumed to be a record of an imaginary wave propagating horizontally with a constant velocity. This assumption is for the sake of the design technique and disagrees with the major opinion that the shear wave propagating upwards from the base rock is predominant in an earthquake motion at the ground surface.

(3) The displacement transfer ratio can be calculated by statically treating the tunnel as a beam in an elastic medium.

The 2nd precondition mentioned above is thought to result in the conclusion that the design method using the spectra is a short of the upper limit design method if the shear wave velocity of the surface layer is taken, because of the following reasons;

(1) Provided that the amplitude is same, the shorter the wave length of a wave propagating in the ground, higher the stress induced in the structure, in other words, the smaller the wave velocity, the higher the stress.

(2) As one of the general properties of wave motion, a wave having long wave length is scarcely disturbed by small obstacles. Therefore long waves propagating upwards from the base rock will generate little disturbance of short period in the surface layer and the apparent wave length of the disturbance due to reflection or refraction by geological and topographical irregularity may have some relationship with that of the incident wave from the base rock.

(3) From more microscopic point of view, phase difference in a surface layer is caused by the occasions that disturbances are generated due to geological or topographical irregularity in the surface layer and propagate horizontally and that some irregularities of base rock result in different travel paths of the wave propagating from the base rock to the surface layer, except to the surface wave. For the former occasion, if only the horizontally propagating shear wave is considered, its velocity must be the shear wave velocity depending upon the property of the layer through which the wave propagates. For the latter, even in the extreme condition shown in Fig. 1, in which the motion of the base rock is

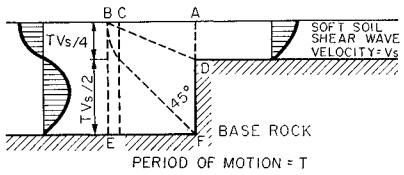

Fig. 1 Illustration of Irregular Base Rock.

assumed in the normal direction to the figure plane, the phase changes gradually in the distance between the points A and B, because the motion of an element in the oscillating medium is governed mainly by the motion of the nearest point of the base rock. The distances from each

point on the line BF to the point D and E in Fig. 1 are equal, and the distance from A to B is longer than the distance from A to C which is a half of the wave length calculated from the period of the motion multiplied by the shear wave velocity. Consequently, an apparent wave length is longer than that calculated by using the shear wave velocity.

(4) With respect to surface waves, the propagation velocity of Love wave is greater than the shear wave velocity of the surface layer.

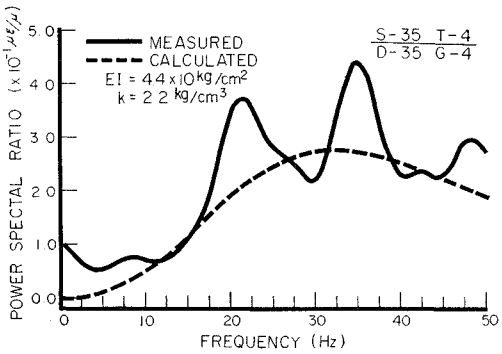

Fig. 2 Result of Dynamic Model Test.

Authors[7] have done a field vibration model test of tunnel. According to the test result, of which an example is shown in Fig. 2, though a resonant phenomenon was observed, it was because the frequency of the excitation vibration was very high, and prototype tunnels will scarcely resonate with earthquakes, considering similitude. And also it was found that the response of the model to the shear wave propagating horizontally can be explained by assuming the model as a beam in an elastic medium and by static calculation, as is shown in Fig. 2.

3. COMPUTATION OF DESIGN SPECTRA

It has previously mentioned that the displacement transfer ratio can be statically calculated by assuming the tunnel as a beam in an elastic medium. From the theory of elasticity, the following basic equation is obtained, taking the tunnel axis for x-axis.

$$EI\frac{d^4u_t}{dx^4}=K(u-u_t) \quad \cdots\cdots(1)$$

where EI, K, u and u_t stand for the bending rigidity of the tunnel, the spring constant of soil, the displacement of soil in the transverse direction of x-axis and the displacement of the tunnel in the same direction as soil. Taking sinusoidal waves of amplitude of U and U_t for the displacement of soil and the tunnel respectively, that is, $u=U\sin 2\pi x/L$ and $u_t=U_t\sin 2\pi x/L$, and substituting into eq. (1), the displacement of the tunnel without boundary is obtained as follows;

$$u_t=\frac{u}{\frac{EI}{K}\left(\frac{2\pi}{L}\right)^4+1}=\frac{U}{\frac{EI}{K}\left(\frac{2\pi}{L}\right)^4+1}\sin\frac{2\pi}{L}x \quad \cdots\cdots(2)$$

where L is the wave length of the ground displacement. Supposing the ground displacement wave propagates with a velocity of V_s, the wave length, L can be replaced by V_sT and x by V_st, where T is the period of the propagating ground displacement wave and t is time. Substituting these relations into eq. (2), eq. (3) is obtained.

$$u_t=\frac{U}{\frac{EI}{K}\left(\frac{2\pi}{V_s}\right)^4\frac{1}{T^4}+1}\sin\frac{2\pi}{T}t \quad \cdots\cdots(3)$$

Introducing the following quantity.

$$\tau=\frac{2\pi}{V_s}\sqrt[4]{\frac{EI}{K}} \quad \cdots\cdots(4)$$

let us call it "rigidity ratio period". This value, τ is unique for a tunnel and depends upon the rigidity of the tunnel and soil and has a dimension of time and indicates a characteristic of the tunnel like the natural period of a system. Using eq. (4), eq. (3) can be reduced as eq. (5).

$$u_t=G(\tau, T)u=\frac{U}{(\tau/T)^4+1}\sin\frac{2\pi}{T}t \quad \cdots\cdots(5)$$

where $G(\tau, T)=1/(\tau^4/T^4+1)$ is the transfer function of the displacement from the ground to the tunnel, which depends on the rigidity ratio period and the period of the wave propagating in the ground.

The curvature, ρ of the tunnel which is deformed into the sinusoidal shape can be represented as follows;

$$\rho=\frac{d^2u_t}{dx^2}=\frac{1}{V_s^2}\frac{d^2u_t}{dt^2}$$

$$=-G(\tau, T)U\left(\frac{2\pi}{T}\right)^2\frac{1}{V_s^2}\sin\frac{2\pi}{T}t \quad \cdots\cdots(6)$$

The relation between the amplitude of the displacement, U, and the acceleration, a, of a sinusoidal wave is $a=(2\pi/T)^2U$, then eq. (6) can also be rewritten as eq. (7).

$$\rho V_s^2=-G(\tau, T)\cdot a\cdot\sin 2\pi t/T \quad \cdots\cdots(7)$$

On the other hand, an accelerogram of an earthquake can be represented in a Fourier series, as follows;

$$a_e(t)=\sum_n a_n\cdot\sin\{(2\pi t/T_n)+\phi_n\} \quad \cdots\cdots(8)$$

where $a_e(t)$ is the acceleration of the earthquake, ϕ_n is the phase angle and the suffix n stands for the nth term of the series. Because eq. (7) can be applicable for each component of the Fourier amplitude represented by eq. (8), the curvature induced in a tunnel by an earthquake can be formulated as eq. (9).

$$\rho V_s^2 = -\Sigma G(\tau, T_n)\cdot a_n \cdot \sin\left(\frac{2\pi}{T_n}t+\phi_n\right) \cdots (9)$$

Eq. (9) can easily be computed by an electronic computer for a digitized accelerogram and for various value of τ. The computing process is shown in Fig. 3. The top row shows the $N-S$

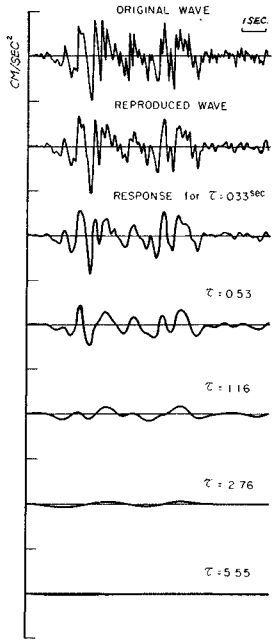

Fig. 3 Computing Process of Design Spectrum.

component of the El Centro earthquake for the first 10 seconds. The wave in the 2nd row is the reproduced wave by such a way that the original wave is expanded into a Fourier series in the range of 0.15—10 seconds of period then the components are again superimposed taking the phase angle into consideration. Two waves, the original and the reproduced coincide fairly good, though the high frequency components seem to be lost because the record of the El Centro earthquake has comparatively high frequency components. The components of the period less than 0.15 seconds have been neglected, considering the computing time and the fact that such high frequency component has scarcely influence on the design of tunnels. Each row below the 2nd row shows the computation results of eq. (9) for $\tau=$ 0.33, 0.53, 1.16, 2.76, and 5.55 seconds in turn. It is nicely illustrated that the transfer ratio becomes smaller and smaller as the rigidity of the structure becomes larger and larger. Fig. 4 shows the Fourier amplitude spectra of the waves in Fig. 3. It can be seen that the high frequency components become smaller as τ increases.

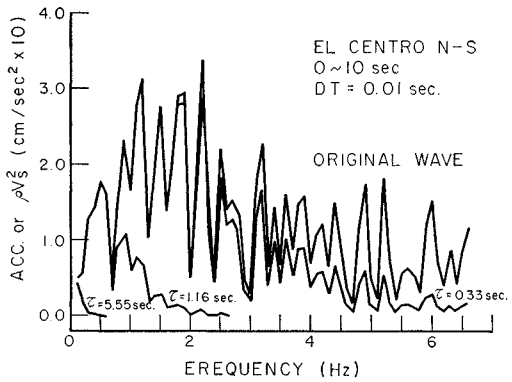

Fig. 4 Fourier Spectrum of EL Centro Earthquake and Curvature Response.

The maximum value of ρ can be taken out of each wave lower than the 2nd row of Fig. 3. Repeating this process for many various values of τ, a design spectrum can be obtained for bending of tunnels as a function of the rigidity ratio period, τ. Letting $H_\rho(\tau)$ be the spectrum obtained by above process, eq. (10) is obtained.

$$H_\rho(\tau) = |\rho V_s^2|_{\max} = \left|\Sigma G(\tau, T_n)\cdot a_n \cdot \sin\left(\frac{2\pi}{T_n}t+\phi_n\right)\right|_{\max} \cdots (10)$$

Let us call $H_\rho(\tau)$ the "curvature response spectrum". $H_\rho(\tau)$ has a dimension of acceleration. Fig. 5 shows the curvature response spectrum of the $N-S$ component of the El Centro earthquake modified to 100 gal. of the maximum acceleration.

Recalling that eq. (6) gives us the curvature induced in the tunnel by a single sinusoidal wave, the relationship between the displacement amplitude and the period which gives us the same maximum curvature induced as that calculated from an earthquake can be obtained by substituting eq. (6) into eq. (10).

$$U = \frac{|\rho V_s^2|_{\max}}{G(\tau, T)}\left(\frac{T}{2\pi}\right)^2 = \frac{H_\rho(\tau)}{G(\tau, T)}\left(\frac{T}{2\pi}\right)^2 \cdots (11)$$

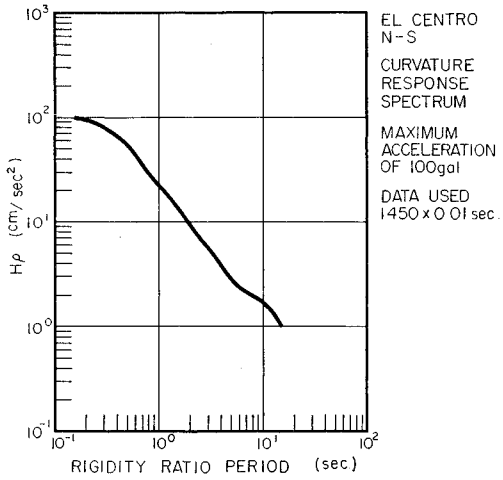

Fig. 5 Curvature Response Spectrum.

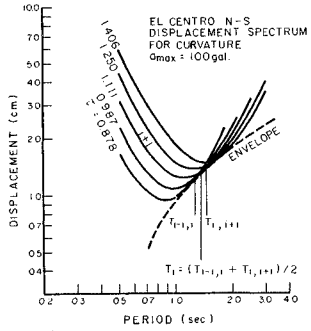

Fig. 6 Relation between Displacement 8 Period.

Eq. (11) represents a group of curves which are concave upwards on the $U-T$ coordinate as shown in Fig. 6. Taking a curve for a particular value of τ, U and T on every points along the curve gives us the same curvature induced in the tunnel which is the maximum calculated from the earthquake the curve has been computed from. An envelope of the group of the curves can be drawn as shown in Fig. 9. This envelope has following characteristics. If the curvature induced in the tunnel is calculated for $\tau=\tau_0$ from U and T along the envelope, U and T on the point where the envelope is in contact with the curve represented by eq. (11) for $\tau=\tau_0$ gives us the maximum curvature and which is equal to that induced by the earthquake the curves calculated from, and the curvature lated with U and T on the other point of the envelope is always smaller. Provided that the calculation of the curvature in the practical design is done by such a way that the maximum curvature is looked after by picking up the values of U and T on the envelope along it, this envelope can be used as the design displacement spectrum for curvature. Let us call the envelope the "displacement amplitude spectrum of equivalent sinusoidal wave for curvature", which is a function of only the period of the ground motion, T.

Numerical computation of the envelope can be executed as follows; letting $T_{i-1,i}$ be the intersect of the curves represented by eq. (11) for $\tau=\tau_{i-1}$ and $\tau=\tau_i$ eq. (12) is obtained,

$$T_{i-1,i}=\frac{H(\tau_i)\tau_{i-1}^4-H(\tau_{i-1})\tau_i^4}{H(\tau_{i-1})-H(\tau_i)}\,,$$

$$H(\tau_{i-1})-H(\tau_i)>0 \quad \cdots\cdots\cdots\cdots(12)$$

In the same manner, $T_{i,i+1}$ can be gotten. The displacement amplitude, U, obtained by substituting the average value of $T_{i-1,i}$ and $T_{i,i+1}$, $T_i=(T_{i-1,i}+T_{i,i+1})/2$, into eq. (11) with $\tau=\tau_i$ is considered to be the displacement amplitude for the period of T_i, as shown in Fig. 6. That $H(\tau_{i-1})-H(\tau_i)$ is equal or less than zero means two curves for $\tau=\tau_i$ and $\tau=\tau_{i-1}$ has no intersect at least in the positive zone of the period. In such rare case, the envelope must be deformed so that the envelope has a common point with all curves represented by eq. (11), considering the application purpose. As a result of above mentioned treatment the spectrum deformed gives us a slightly larger displacement than that calculated by eq. (11) for some values of τ. On Fig. 7, the

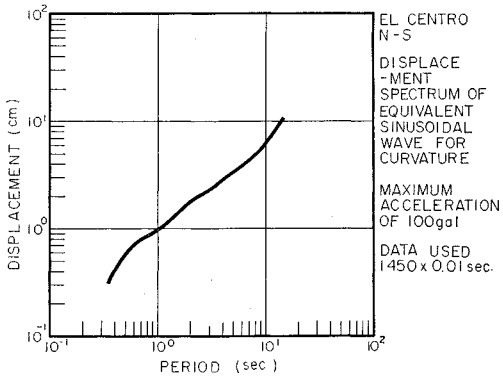

Fig. 7 Displacement Spectrum for Curvature.

displacement amplitude spectrum of equivalent sinusoidal wave for curvature of the $N-S$ component of the El Centro earthquake is shown.

Bending problems of tunnels have been discussed so far and the corresponding spectra have been led with examples illustrated. By the same manner, spectra for the shear force, the load in

the transverse direction to the tunnel axis, the axial strain and the axial load can be obtained.

For the shear force, following equation is led from eq. (5).

$$S=-EI\frac{d^3u_t}{dx^3}=-\frac{EId^3u_t}{V_s^3dt^3}$$
$$=G(\tau,T)\cdot U\cdot\left(\frac{2\pi}{T}\right)^3\frac{EI}{V_s^3}\cos\frac{2\pi}{T}t \quad\cdots\cdots(13)$$

Then,

$$H_s(\tau)=\left|\frac{SV_s^3}{EI}\right|_{\max}$$
$$=\left|\sum_n G(\tau,T_n)a_n\cdot\left(\frac{2\pi}{T_n}\right)\cos\left(\frac{2\pi}{T_n}t+\varphi_n\right)\right|_{\max}$$
$$\cdots\cdots(14)$$

where $H_s(\tau)$ is called the shear response spectrum. From eqs. (13) and (14), the displacement amplitude spectrum of the equivalent sinusoidal wave for shear is obtained as an envelope of the group of curves represented by eq. (15).

$$U=\left|\frac{SV_s^3}{G(\tau,T)EI}\right|_{\max}\left(\frac{T}{2\pi}\right)^3$$
$$=\frac{H_s(\tau)}{G(\tau,T)}\left(\frac{T}{2\pi}\right)^3 \quad\cdots\cdots(15)$$

For the lateral load, corresponding spectra are obtained from following equations.

$$H_{pl}(\tau)=\left|\sum_n G(\tau,T_n)\cdot a_n\cdot\left(\frac{2\pi}{T_n}\right)^2\sin\left(\frac{2\pi}{T_n}t+\varphi_n\right)\right|_{\max} \quad\cdots(16)$$

$$U=\frac{H_{pl}(\tau)}{G(\tau,T)}\cdot\left(\frac{T}{2\pi}\right)^4 \quad\cdots\cdots(17)$$

With respect to the axial displacement, because the force transmitted from soil to the tunnel can not exceed the friction between them, there is a limitation only within which the spring constant of soil is considered to be elastic. It is assumed in the following discussion that the relative displacement between soil and the tunnel is within the limitation mentioned above. In the practical application of the spectra, therefore, it must be checked whether the axial load exceeds the friction between soil and the tunnel or not. If the axial load is found to be greater than the friction force, it must be taken into consideration. Letting K' be the spring constant of soil in the direction of the tunnel axis, L' be the apparent wave length, V' be the apparent wave velocity, u' be the component of the ground motion in the direction of the tunnel axis and u_t' be that of the tunnel, and taking the tunnel axis for x-axis, the basic equation is as follows;

$$AE\frac{d^2u_t'}{dx^2}=K'(u'-u_t') \quad\cdots\cdots(18)$$

where A is the sectional area of the tunnel and E is the Young's modulus of the material the tunnel made of. Taking a sinusoidal wave for the ground motion of an amplitude of U', i.e., $u'=U'\sin(2\pi x/L')$, the displacement of the tunnel without boundary, u_t' is represented by the following equation.

$$u_t'=\frac{u'}{\frac{AE}{K'}\left(\frac{2\pi}{L'}\right)^2+1}$$
$$=\frac{U'}{\frac{AE}{K}\left(\frac{2\pi}{L'}\right)^2+1}\sin\frac{2\pi}{L'}x \quad\cdots\cdots(19)$$

By the same manner as done in the bending problem discussed previously, substituting the Fourier expression of accelerograms, corresponding spectra can be obtained as follows.

For the axial strain, ε,

$$H_\varepsilon(\tau')=\left|\sum_n G'(\tau',T_n)\cdot a_n\cdot\frac{T_n}{2\pi}\cdot\cos\left(\frac{2\pi}{T_n}t+\varphi_n\right)\right|_{\max} \quad\cdots\cdots(20)$$

and

$$U=\frac{H_\varepsilon(\tau')}{G'(\tau',T)}\left(\frac{T}{2\pi}\right) \quad\cdots\cdots(21)$$

where $G'(\tau',T)=1/(\tau'^2/T^2+1)$ is the transfer function of the displacement in the axial direction, and $\tau'=(2\pi/V')\sqrt{AE/K'}$ is the rigidity ratio period in the axial direction.

For the axial load, the following equations are obtained.

$$H_{pa}(\tau')=\left|\sum_n G'(\tau',T)\cdot a_n\cdot\sin\left(\frac{2\pi}{T_n}t+\varphi_n\right)\right|_{\max} \quad\cdots\cdots(22)$$

$$U=\frac{H_{pa}(\tau')}{G'(\tau',T)}\left(\frac{T}{2\pi}\right)^2 \quad\cdots\cdots(23)$$

Eqs. (20) and (22) are called the axial strain response spectrum and the axial load response spectrum respectively. And envelopes of eqs. (21) and (23) are called the displacement amplitude spectra of equivalent sinusoidal wave for the axial strain and the axial load respectively. When the axial load calculated from the axial load response spectrum is greater than the friction force between soil and the tunnel, it can be considered that a slip occurs between soil and the tunnel and may absorb the relative displacement by the slip, then such a large strain that is obtained from the axial strain response spectrum can not

be induced during the earthquake. On Figs. 8-10, the shear response spectrum, the axial strain response spectrum and the axial load response spectrum of the $N-S$ component of the El Centro

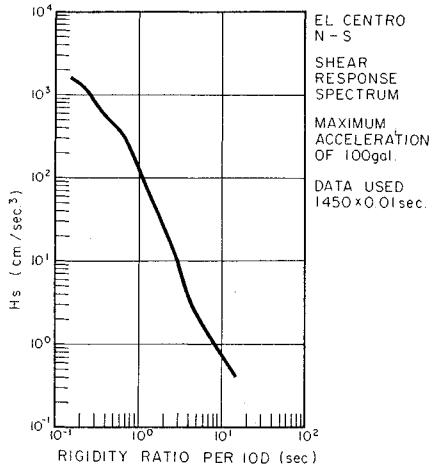

Fig. 8 Shear Response Spectrum.

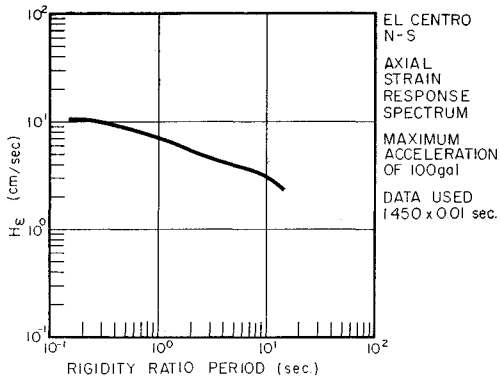

Fig. 9 Axial Strain Response Spectrum.

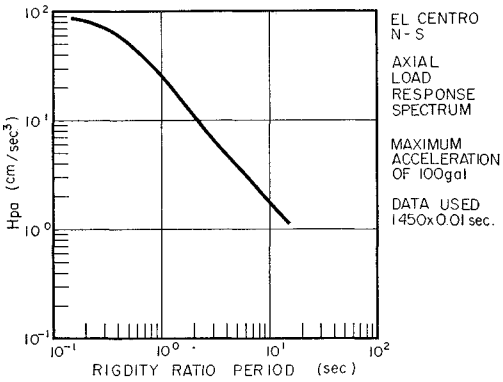

Fig. 10 Axial Load Response Spectrum.

earthquake are shown. On Fig. 11, five displacement amplitude spectra of equivalent sinusoidal wave are shown. At a glance, five spectra are able to be classified into two groups; the first includes those connected with the displacement in the transverse direction of the tunnel axis and the other includes those in the axial direction. From the practical point of view, each group seems to be represented by a single curve, because the spectra in each group are plotted in a narrow range.

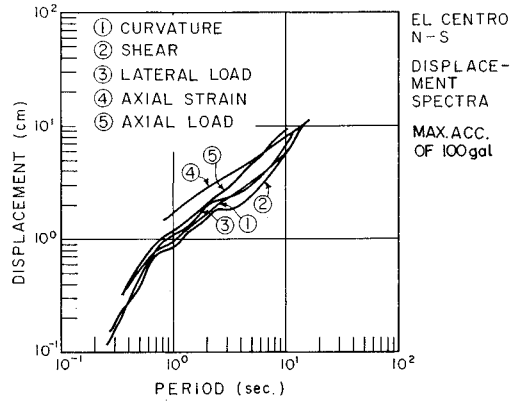

Fig. 11 Displacement Spectra.

4. FORMULATION OF THE PROBLEM AT JOINTS BETWEEN TUNNEL TUBE AND VENTILATION TOWER

The design of joints between the tube and the ventilation tower is in general more important problem rather than tunnel tubes themselves in the earthquake-resistant design of trench type tunnels. According to the following way of thinking, the bending moment or the curvature at a rigid joint or the relative displacement at a flexible joint between a tunnel tube and a ventilation tower can be calculated from the spectra obtained previously.

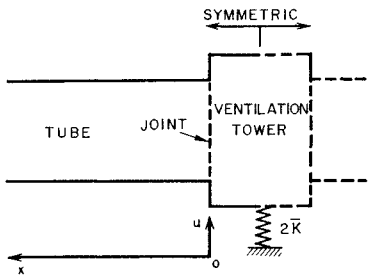

Fig. 12 Calculation Model of Joint (Plant).

As shown in Fig. 12, taking the end of the tube for the origin of the x-axis and it is assumed that the ventilation tower is rigid and the tunnel is symmetric with respect to the center of the ventilation tower. Therefore the ventilation tower will not rotate arround the vertical axis at the instance that the maximum displacement in the transverse direction occurs at the tower. Letting $2\bar{K}$ be the lateral spring constant of the tower, which has defferent dimension from K or K'. Though eq. (2) have been obtained for a infinitely long beam without boundary, the following boundary conditions are adapted in this case by taking the above mentioned assumptions into consideration.

$$\left(\frac{du_t}{dx}\right)_{x=0}=0 \quad \text{and} \quad S_{x=0}=-\bar{K}(u-u_{bt}) \qquad \cdots\cdots(24)$$

where u_b, is the displacement of the ventilation tower. Taking $u=U\cos(2\pi x/L)$ for the ground motion, which gives us the maximum displacement at $x=0$, and considering the condition that the influence of the boundary disappears at $x=\infty$, the following equation is a solution of eq. (1).

$$u_t=G(\tau, T)\cdot U\cdot\cos\frac{2\pi}{L}x + e^{-\beta x}(C\cos\beta x+D\sin\beta x) \qquad \cdots\cdots(25)$$

where $\beta=\sqrt[4]{K/4EI}$ and C and D are constants which are determined from the boundary conditions of eq. (24) as follows.

$$C=D=\frac{U\{1-G(\tau, T)\}}{1+4EI\beta^3/\bar{K}} \qquad \cdots\cdots(26)$$

Substituting eq. (26) into eq. (25), the displacement of the tunnel near the joint can be obtained.

$$u_t=G(\tau, T)\cdot U\left\{\cos\frac{2\pi}{L}x + \frac{\tau^4}{T^4(1+4EI\beta^3/\bar{K})}(\cos\beta x+\sin\beta x)\right\} \qquad \cdots\cdots(27)$$

Then the curvature at the joint can be formulated as follows.

$$\left(\frac{M}{EI}\right)_{x=0}=\left(\frac{d^2u_t}{dx^2}\right)_{x=0} =G(\tau, T)U\left\{\left(\frac{2\pi}{L}\right)^2+\frac{2\tau^4\beta^2}{T^4(1+4EI\beta^3/\bar{K})}\right\} \qquad \cdots\cdots(28)$$

With respect to the flexible joint, assuming that no forces are transmitted across the joint, the following boundary conditions are adapted.

$$M_{x=0}=0 \quad \text{and} \quad S_{x=0}=0 \qquad \cdots\cdots(29)$$

The constants in eq. (25) are determined from the above conditions as follows.

$$C=-D=\frac{U}{2\beta^2}G(\tau, T)\cdot\left(\frac{2\pi}{L}\right)^2 \qquad \cdots\cdots(30)$$

Then substituting the constants into eq. (25), the displacement of the tube near the joint is obtained as follows;

$$u_t=G(\tau, T)\cdot U\left\{\cos\frac{2\pi}{L}x + \frac{1}{2\beta^2}\left(\frac{2\pi}{T}\right)^2 e^{-\beta x}(\cos\beta x-\sin\beta x)\right\} \qquad \cdots(31)$$

Therefore assuming that the ventilation tower moves equally with the surrounding ground, the relative displacement, δ, at the flexible joint can be represented by eq. (32).

$$\delta=U-(U_t)_{x=0}=U\cdot G(\tau, T)\{(\tau/T)^4-2(\pi/\beta L)^2\} \qquad \cdots\cdots(32)$$

The curvature at the rigid joint, eq. (28) and the relative displacement at the flexible joint, eq. (32) are expressed in the forms of the displacement of the ground motion multiplied by a sort of frequency transfer function. Therefore these values can be computed directly from an accelerogram. Considering that this method is a tentative one and based on the bold assumptions, it is, however, not adequate to make a minute calculation. The calculation using the displacement amplitude spectrum for curvature obtained previously is enough for the practical design.

The problems in the axial direction can also be treated in the same manner as in the transverse direction discussed above with paying an attention to the fact that the problem about the friction is involved. In this paper, however, the problems in the axial direction will not discussed any more, because little experimental study has been done and important problems such as the determination of the spring constant in the axial direction and the transmission of displacements and forces along the axis associate with the friction have been left unclearified.

5. EXAMPLES OF APPLICATION

The computation method of the design spectra and the method of the prediction of the curvature induced at a rigid joint and the relative displacement at a flexible joint between a tunnel tube and a ventilation tower are discussed in the previous sections. How the design spectra and the prediction method of the curvature and the relative displacement at the joint work will be concretely illustrated in this section. Two examples are taken; one of them is such a case

that the ground is hard and the rigidity of the tunnel is comparatively small, and the other is a rigid tunnel in a soft ground contrariwise. The former, example 1, is the Kinuura port tunnel which is under construction in Handa city, Aichi prefecture and the latter, example 2, is an imaginary tunnel. The spectra of the $N-S$ component of the El Centro earthquake shown on the Fig. 5 and Figs. 7-11 are applied for the above mentioned two examples. The results of the example 1 will be compared with the values of the design which was done in the past.

Table 1 Application examples.

Items	Example 1	Example 2
Rigidity, EI (kg-cm^2)	2.3×10^{16}	3.5×10^{17}
Sectional Area, A (m^2)	42.85	61.2
Width, B (m)	15.6	37.4
S-wave Velocity, V_s (m/sec)	250	100
Rigidity Ratio Period, τ (sec)	0.33	3.0
Rigidity Ratio Period, τ' (sec)	0.97	—
Curvature Resp., H_ρ (cm/sec^2)	66	5
Curvature, $\rho=H_\rho/V_s^2$ (1/cm)	10.6×10^{-8}	5×10^{-8}
Fiber Strain, $\varepsilon=\rho B/2$ ($\mu\varepsilon$)	90	93.5
Shear Resp., H_s (cm/sec^3)	630	9.5
Shear Force, $S=EI\,H_s/V_s^3$ (kg)	9.3×10^5	3.3×10^6
Axial Strain Resp., H_ε (cm/sec)	8.5	—
Axial Strain*, $\varepsilon=H_\varepsilon/2V_s$ ($\mu\varepsilon$)	170 (200)	—

* Shear wave with incident angle of 45° is assumed. The number in bracket stands for the case which rigidity ratio period goes down extremely.

At first the calculation for the tunnel tube itself will be shown. The results are listed in the Table 1. The rigidity ratio period in the transverse direction is 0.38 sec. and that in the axial direction is approximately 1 sec. for example 1. For example 2 it is 3 sec. in the transverse direction. The rigidity ratio period in the axial direction for example 2 will be abbreviated. The rigidity ratio period of example 1 belogns to the very short group and that of example 2 is comparatively long one. Because the spectra used have been normalized for the earthquake of the maximum acceleration of 100 gal., the values in Table 1 are also for the earthquake of 100 gal. of the maximum acceleration. The bending strain induced in the tunnels are not different, though the curvature induced in the tunnel of example 2 is twice of that of example 1. The shear force induced in the tunnel of example 2 is considerably large. If the design acceleration is assumed to be 250 gal., the shear force of 8,250 tons must be considered. Assuming that 80% of the sectional area of concrete is effective against the shear force, the shear stress of 16.8 kg/cm^2 is obtained. Considering that the main reinforcing bars in the cross section work against the diagonal tension, the tunnel is, however, not unsafe against shear failure. The shear force for example 1 is small enough.

There are two kinds of waves which are considered to induce the axial strain in tunnels. One of them is the wave of dilatation propagating in the direction of the tunnel axis and the other is the wave of distortion which propagates with some angle to the tunnel axis. The axial strain response spectrum and the axial force response spectrum obtained previously can be applied for both case. When a wave of dilatation is considered, the wave velocity of the wave of dilatation is taken for V'. And when a wave of distortion is considered, the shear wave velocity projected on the tunnel axis must be taken, and the axial force and the axial strain obtained from the spectra also must be projected on the tunnel axis. When the wave of distortion with an incident angle of 45° is considered, the axial strain induced is in general greater than that induced by the wave of dilatation. For the wave of distortion with an incident angle of 45°, $\sqrt{2}\,V_s$ can be taken for V'. And the strain and the force multiplied by $\sqrt{2}$ are those required. The strain of 170 $\mu\varepsilon$ is obtained for the tunnel of example 1. Because the spectrum used is for the earthquake of the maximum acceleration of 100 gal., assuming 250 gal. for the design acceleration the axial strain induced becomes 425 $\mu\varepsilon$. The structural concrete of the tunnel will break in a such high strain and only steel members carry the force. In this case the axial rigidity of the tunnel goes down and consequently the rigidity ratio period become small. Assuming even a zero rigidity ratio period for an extreme case, the strain induced in the tunnel goes up at most 200 $\mu\varepsilon$ for 100 gal. of the maximum acceleration, then 500 $\mu\varepsilon$ for 250 gal., which is safe enough comparing with the ductility of steel and materials for the water proof works. This is because of the limitation of the displacement of the ground motion during the earthquake.

The force which induces strains in the tunnel is transmitted from the surrounding soil by the

friction force between the tube and the soil. For the example 1, the axial force of 3,000 kg/cm is calculated from the spectrum. Assuming that this force is transmitted through the area of the bottom and a half of side walls of the tunnel, the transmitting force through a unit surface area of the tunnel is 1.3 kg/cm². Considering that the effective stress calculated from the overburden pressure at the bottom of the tunnel is less than 1.0 kg/cm², the slip between the tunnel and soil may occur and such large force calculated directly from the spectrum will not transmitted to the tunnel. Therefore, as mentioned previously, the strain calculated above must be made some modification.

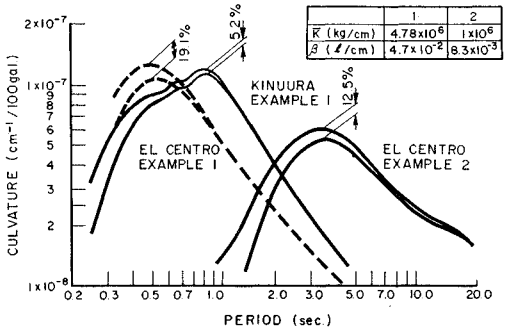

Fig. 13 Curvature at Rigid Joint.

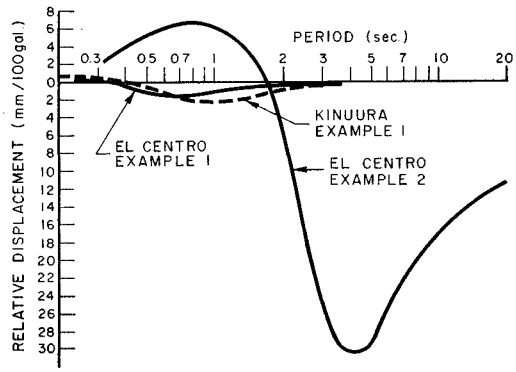

Fig. 14 Relative Displacement at Flexible Joint.

Examples of the application of the prediction method for the curvature induced at the rigid joint and the relative displacement at the flexible joint between the tube and the ventilation tower are shown on Figs. 13 and 14 respectively. For the $N-S$ component of the El Centro earthquake, the curvature at the rigid joint increases 19.1% for example 1 and 12.5% for example 2 compared with those induced in the tube located far enough from the joint at the period of the ground motion which gives us the maximum curvature. The increment ratio of the curvature at a rigid joint becomes greater when the rigidity of a tunnel becomes higher if the same period of a ground motion is assumed. But in these examples the periods of the ground motion which cause the maximum curvature are quite different each other, and as a result the increment ratio for example 1 was greater than the other. If the displacement spectrum which has been used in the past design is applied for the tunnel of example 1, the period of the ground motion which cause the maximum curvature becomes larger and the increment ratio of the maximum curvature drops down up to 5.2% as shown on Fig. 13.

Fig. 14 shows the relationship between the relative displacement at the flexible joint and the period of ground motion. One of a characteristics of this figure is that the sign of the relative displacement turns out inverse at a certain value of period of the ground motion. This is understandable by the following reasons. When the period of the ground motion is long comparing with the rigidity ratio period of the tunnel, the tube and the ventilation tower oscillate in a same amplitude and then the phenomenon that the free end of the tunnel swings out dominates the relative displacement, and when the period of the ground motion is short, the displacement of the tube end will be smaller than that of the ventilation tower due to the rigidity of the tube.

The amounts of the relative displacement at the flexible joints for the tunnels taken as examples are calculated to be 1.5 mm for the tunnel of example 1 and 32 mm for the tunnel of example 2 for the $N-S$ component of the El Centro earthquake. These values are for 100 gal. of maximum acceleration. The relative displacement at the flexible joint of the tunnel of example 1 for the displacement spectrum which has been used for its past design is calculated to be 2.2 mm by this method.

According to the results of the application examples of the prediction method of the curvature at a rigid joint and the relative displacement at a flexible joint between a tube and a ventilation tower, it seems that a flexible joint is more effective for tunnels with high rigidity than tunnels with low rigidity.

The tunnel taken as example 1 has already been designed and under construction at the port of Kinuura, Handa city, Aichi prefecture. The key values connected with the earthquake-resistant design of the past design already done are

Table 2 Comparison with past design.

Items	New spectra	Past design
Bending moment (t-m)	6.10×10^4	6.25×10^4
Shear force (t)	2.32×10^3	2.47×10^3
Axial force (t)	3.82×10^4	2.63×10^4

listed in Table 2 together with those obtained from the spectra of the $N-S$ component of the El Centro earthquake, both for 250 gal. of the maximum acceleration. Both the curvature and the shear force do not make any difference. The axial force calculated from the spectrum of the El Centro earthquake obtained in this paper result to be slightly larger than that of the past design.

6. CONCLUSIONS

The earthquake-resistant design method of tunnels constructed by the trench method which utilizes design spectra is one of the superior methods from the practical point of view, because of the following reasons. That is, provided that the spectra have been prepared in advance, this design method is quite simple in prosecution, and this design method presumably gives us the upper limit value which covers unknown factors. A new computation method of the design spectra is proposed in this paper.

A tentative method for the prediction of the curvature induced at a rigid joint and the relative displacement at a flexible joint between a tube and a ventilation tower is also proposed. This problem is in general more important than the design of tudes themselves independent of the joint. It has been shown that for this method of prediction the design spectra proposed in this paper can be utilized.

Taking two extremely different types of tunnels for examples the application of the spectra obtained by the method proposed and the proposed method of the prediction of the preblems connected with a joint between a tube and a ventilation tower have been illustrated. The results of the examples were quite understandable.

The author is planning to compute the spectra for many available strong motion accelerograms and classify them into a few groups with consideration of the ground conditions at which the accelerograms were recorded and prepare a set of design spectra for each group by means of some statistical treatments.

ACKNOWLEDGEMENT:

Dr. Hayashi, head of the Structures Division, and Mr. Tsuchida, chief of the Earthquake Resistant Structure Laboratory, made constructive comments on a draft of this paper. Mr. Maruyama, member of the Materials Laboratory helped in computation of spectra illustrated.

REFERENCES

1) Tamura, C. and Okazaki, T.: Dynamic Model Test of Trench Type Tunnel, Preprint of 11th Earthquake Engineering Symposium on Civil Engineering Structure, pp. 29-32, July, 1971.
2) Muto, K., Uchida, K. and Tsugawa, T.: The Earthquake Response Analysis of Underground Tunnels, Proc., 3rd Japan Earthquake Engineering Symposium, pp. 437-444, Nov., 1970.
3) Hamada, M.: Earthquake Response Analysis of Trench Type Tunnels, Preprint of 26th Annual Conference of JSCE, pp. 317-320, Oct., 1971.
4) Goto, Y., Ohta, J. and Sato, T.: Earthquake Analysis of Trench Type Tunnels by F.E.M., Preprint of 26th Annual Conference of JSCE, pp. 321-324, Oct., 1971.
5) The San Francisco Bay Area Rapid Transit Commission: Technical Supplement to the Engineering Report, 1960, July. (Translated in Japanese by the Public Works Research Institute, Oct., 1968)
6) Sakurai, A.: Earthquake Resistivity of Underground Pipelines, Preprint of Regional Symposium of JSSMFE, Hokkaido Branch, Oct., 1970.
7) Aoki, Y., Tsuchida, H. and Hayashi, S.: Outdoor Dynamic Model Test of Trench Type Tunnel, Preprint of 11th Earthquake Engineering Symposium on Civil Engineering Structures, pp. 21-24, July, 1971.

(*Received March 23, 1972*)